Silicon (2024) 16:5243–5256
https://doi.org/10.1007/s12633-024-03079-5

RESEARCH

Formulation and Characterization of Silane Modified Acrylic Based Transparent Organic-Inorganic Hybrid Coatings for Improved Instrumented Indentation Hardness of PMMA

Vishal Das[1] · Ajit Shankar Singh[1] · Abhishek Singh[1] · Preeti Mishra[1] · Dibyendu Sekhar Bag[1]

Received: 15 October 2023 / Accepted: 23 June 2024 / Published online: 2 July 2024

Abstract
Acrylic substrates made from polymethylmethacrylate (PMMA) are anticipated to develop craze and scratches owing to their continual wear. In this study, novel silane modified acrylic resin based organic-inorganic hybrid coating materials have been formulated to provide protection to PMMA substrates against wear. Varied amounts (5, 10 and 15 % wt./wt.) of tetraethoxysilane (TEOS) were added to the acrylic resin solution (containing xylene and 10% ammonia) and the resultant hybrid coating materials were then coated on PMMA substrates through the dip coating method. The hybrid coating materials were transformed into hard coats upon hydrolysis, condensation and cross-linking. The coated samples were characterized to assess the effect of TEOS addition on optical and mechanical properties as well as abrasion resistance of the hybrid coatings. Hardness, stiffness and reduced elastic modulus of the dry coatings obtained through the instrumented indentation technique were observed to increase (up to ca. 56%, 28% and 65% respectively) whereas their viscous nature and plasticity decreased with the addition of TEOS. The hybrid coatings also demonstrated improved wet abrasion resistance which augurs well with their physico-mechanical properties. These observations can be ascribed to the combined contributions of organic-inorganic phase interactions in the coating materials via hydrogen bonding and the formation of cross-linked silica structures as observed through infrared spectroscopy and microscopy.

Keywords PMMA · Coating · TEOS · Transmittance · Instrumented indentation

1 Introduction

Over four decades, transparent polymeric materials have been utilized as windows in aircraft, buildings and optical lenses due to their better flexibility, exceptional impact resistance, lighter weight and equivalent transparency as compared to glass. Polymethylmethacrylate (PMMA) and Polycarbonate (PC) are the most prominently used optically transparent polymers for automobile and civil applications owing to their high transparency, low density, ability to be processed into various shapes and high impact strength [1]. Most of the windows, visors, screen and protective goggles, etc. are made from acrylic (PMMA) sheets which are cast to impart mirror-like surface finish. However, the deterioration of acrylic sheets is mainly because of the development of crazes and scratches during routine operational usage due to its poor scratch resistance owing to which the transparency is significantly impaired. Thus, to avert the propensity of replacing the worn-out acrylic based transparent windows, visors and screen, protection of the acrylic sheets with a transparent coating is required. Protective coatings based on organic polymers alone are inadequate to meet the long term usage requirements because of their inadequate hardness and wear resistance properties [2]. Consequently, various techniques have been devised by researchers to enhance the hardness and wear resistance properties of the organic coatings with suitable modifications through the incorporation of various functional groups and additives. Different fillers have been utilized primarily for this property modification. Various nanoparticles (such as SiO_2, TiO_2, ZrO_2 and Al_2O_3) have been reported to appreciably improve the coating's scratch and abrasion resistance due to their hardness coupled with high surface areas [3–7]. However, one practical

✉ Vishal Das
vishaldas2911@gmail.com

[1] Polymers and Rubber Division, Defence Materials and Stores Research & Development Establishment, Defence Research & Development Organisation, DMSRDE P.O., G.T. Road, Kanpur 208013, Uttar Pradesh, India

hurdle in using these nanoparticles for coating applications is their improper dispersion in the organic matrix which limits the optical and mechanical properties of the coatings. Alternatively, surface functionalized nanoparticles have been reported to somewhat surmount this problem [8–11]. Nevertheless, the problem of nanoparticle aggregation might still persist during the coating process, even though the particles could be well dispersed in the organic matrix after mixing. This results in deterioration of the ultimate optical and mechanical properties of the coating. Moreover, agglomeration of nanoparticles may also lead to abrupt viscosity variations in the coating formulations which could pose a problem in the coating processes.

Hybrid organic-inorganic transparent coating materials based on in-situ formation of the inorganic domains have also been reported which present the synergistic advantages of both organic and inorganic materials [12–15]. These hybrid materials have been reported to combine the significant properties of their components like high optical transparency, low processing temperatures, thermal stability and easy availability of precursor materials like metal alkoxides, organosilanes as well as the reinforcing nanoparticles. In addition to the metal or silicon alkoxides, which results in the development of an inorganic network after hydrolysis [13], organosilanes are capable of integrating organic moieties which can be polymerized into the final coating. The curing of functional organic groups can be initiated by suitable thermal, chemical or photochemical processes in order to cross-link the whole organic-inorganic system. Owing to the high cross-link density of these hybrid systems, the resultant coatings have much better hardness, and thus, there is a substantial improvement in their scratch and abrasion resistance as compared to those of purely organic coatings [2]. Furthermore, for meeting the demanding requirements of hardness and transparency levels of these transparent coatings, multi-layer coatings have also been reported [16–19]. In these types of multi-layered coatings, the first layer is typically composed of a soft organic or silicone based coating which can adhere well to the acrylic substrate. Subsequently, the next set of layers may be composed of harder metal oxides incorporated silicon based coatings which are generally produced through the plasma enhanced chemical vapor deposition (PECVD) technique [20]. In some cases, alternate layers of soft organic or silicone based coatings and hard coatings may also be employed. However, these types of multi-layered coatings are expensive due to their specialized coating process. As a consequence, the hybrid organic-inorganic coating systems are finding massive industrial use in protecting soft transparent plastics owing to their exceptional match of transparency and adequate mechanical properties coupled with their ease of processing. These rationales have led to the development of varied organic-inorganic coatings based on polymers like polyurethane, acrylics, silicones, epoxy, etc. which can suitably be used to coat the acrylic sheets used in varied personal, automobile and civil applications. Furthermore, judicious selection of chemicals and their synthesis mechanisms may also lead to generation of interlinks between the organic and inorganic phases in addition to the inorganic clusters thus enhancing the hardness and scratch resistance of the hybrid coatings. Research papers on these types of hybrid coatings where interlinks between the inorganic and organic domains have improved the mechanical properties of the hybrid coatings are extremely rare. This is one of the areas where this paper intends to focus.

Furthermore, knowledge about the basic mechanical properties of the protective coating is imperative for predicting the coating's performance under different types of loads. These properties comprise of hardness (H), modulus (E), stiffness (S) and yield strength, to name a few. Indentation methods, predominantly the instrumented indentation tests like micro-indentation and nano-indentation, facilitate the estimation of mechanical properties of the coating to be determined with a small quantity of material. These tests also exemplify the elastic-plastic behavior of materials. Information obtained from these indentation tests is pivotal for envisaging the wear behavior of the coatings when subjected to scratches or abrasive loads. The analysis method most persistently used to acquire the hardness and modulus through instrumented indentation had initially been reported by Doerner and Nix [21]. This analysis method was subsequently improved by Oliver and Pharr later [22]. Though instrumented indentation methods are commonly used for bulk and composite materials but their importance in the evaluation of mechanical properties of coatings as well as thin films are vital as they allow estimation of properties at very low loads and thicknesses. In this work, the mechanical properties of a novel silane modified acrylic based transparent organic-inorganic hybrid coatings were analyzed by means of instrumented indentation also known as depth sensing indentation (DSI) technique [3, 23]. The instrumented indentation method was chosen as it provides a convenient technique to comprehend the influence of inorganic phase as well as interlinks between the organic and inorganic domains, on hardness, modulus, stiffness and viscoelastic properties of this novel type of hybrid organic-inorganic coatings. Consequently, optical transparency of the prepared hybrid coatings was also correlated with its wet abrasion resistance which was in turn governed by the physico-mechanical properties of the coatings.

2 Experimental Details

2.1 Materials

In order to carry out the present study, 4 mm thick PMMA sheets (A-cast) were obtained from Asia Poly Industrial Sdn

Bhd, Malaysia which were used as substrates. Acrylic resin (KONDICRYL SV 166, 57 wt.% solid resin content) was obtained from Pidilite Industries Limited, India. The schematic chemical structure of the acrylic resin is represented in Fig. 1. Tetraethoxysilane ($Si(OC_2H_5)_4$, TEOS, CAS Number: 78-10-4, reagent grade, 98% purity), iso-propyl alcohol ($(CH_3)_2CHOH$, CAS Number: 67-63-0, 98% purity), ammonia solution (NH_3 sol., CAS Number: 7664-41-7) and xylene ($C_6H_4(CH_3)_2$, CAS Number: 95-47-6, reagent grade, 98% purity) were obtained from Merck and used as received.

2.2 Methods

2.2.1 Coupon Sample Preparation

In this study, PMMA sheets were cut into small samples of dimensions 50 mm X 25 mm by means of a laser cutting machine to ensure accurate and smooth edges of the cut-out pieces. PMMA samples were cleaned using ultrasonic cleaning process to remove dust as well as impurities prior to the application of coatings on it. The PMMA samples were put in a beaker containing the solution of iso-propyl alcohol and distilled water (50:50 vol./vol.). The beaker was then put in the ultrasonic cleaning bath for sonication in order to thoroughly clean the cut-out PMMA samples. After sonication, the PMMA samples were wiped with lint free wipes and dried in an air circulating oven at 60°C for 2 hrs.

2.2.2 Preparation of Coating Formulations

Three different coating solutions of acrylic resin were made each having 20 gm of the resin diluted with 50 ml of xylene in which. 5, 10 and 15% wt./wt. of TEOS with respect to the resin were added to each solution. One blank sample was taken without TEOS addition. 2 - 3 drops of 10% ammonia solution was added to each coating solution containing TEOS and these solutions were then put under magnetic stirring for 2 hrs. The compositions PAC-5, PAC-10 and PAC-15 had TEOS content of 5%, 10% and 15% respectively (wt./wt. with respect to the resin) whereas the composition PAC-0 did not have any TEOS content.

2.2.3 Coating Methodology

PMMA sample specimens which were cleaned in the ultrasonic bath with the solution of iso-propyl alcohol and distilled water earlier were dipped into the coating solution kept in a beaker and held for 30 sec, and then gently pulled up vertically. Adequate 30 sec time was allowed for the coating solution to cover the sample specimens to get a sufficiently thick film after drying. This sufficiently thick coating layer was essential to curtail the contribution of substrate's mechanical properties on the resultant mechanical properties of the coating layer during instrumented indentation. This optimized dip coating process was maintained for all the coating solutions. The dip coated PMMA sample specimens and the uncoated PMMA substrates were then dried at ambient atmosphere for 3 hrs, and then heated at 60°C for 30 min in a vacuum oven.

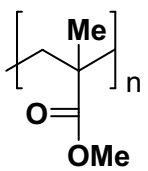

Fig. 1 Schematic of acrylic resin (KONDICRYL SV 166)

2.2.4 Measurement of Physical Properties

Infrared spectra of the samples were recorded on a Perkin Elmer FT-IR RXI spectrophotometer in the range between 4000 and 650 cm^{-1}. The coating film thickness was measured using an AEP NanoMap-D universal surface profilometer. All the coating resin formulations (PAC-0, PAC-5, PAC-10, and PAC-15) were applied onto PMMA sample specimens in three-quarter area for understanding optical as well as thickness difference (so that the coating thickness could be measured easily).

The smoothness and surface morphology of the coating surfaces were observed through a Carl Zeiss EVO 50 scanning electron microscope (SEM). Prior to the SEM analysis, the coated sample specimens were sectioned with the help of a motorized hacksaw and sputter coated with gold powder to observe the surface morphology of the coating under SEM.

The optical transmittances of the uncoated as well as the coated PMMA sample specimens were recorded on an Agilent Cary-60 UV-VIS-NIR spectrophotometer in the wavelength range from 400 nm to 800 nm. Each sample specimens were fixed in the sample mounting window of the UV-VIS-NIR spectrophotometer and the spectrum was recorded directly at various wavelengths.

The wet abrasion tests of the uncoated and the coated PMMA sample specimens were conducted on a TQC Sheen AB6000 scrub abrasion tester in accordance with ASTM D2486. A traverse speed of 60 cycles/min was selected with a stroke length of 50 mm utilizing brush with nylon bristles. The wetting of the sample specimen's surfaces with distilled water and detergent was done through maintaining the pump flow rate at 3 ml/min. The uncoated and coated PMMA sample specimens were subjected to a total of 1200 scrub cycles each during testing. With an intent to quantify the consequence of wet abrasion test on the optical performance of the coatings, transmittance and haze values of the uncoated as well as the coated sample specimens were recorded on a Vista Hazemeter (Hunterlab Instruments, USA) as per ASTM D1003 before and after the wet abrasion tests.

2.2.5 Instrumented Indentation Tests

With the intention of studying the effect of TEOS addition on the mechanical properties of the prepared hybrid organic-inorganic coatings subjected to instrumented indentation, a micro-hardness dynamic indention instrument (CSM Micro-Hardness Tester, CSM Instruments, Switzerland) was utilized. All micro-indentation tests were performed with a Vickers type diamond indenter probe using 10 Hz acquisition rate. A linear indentation loading rate of 60 mN/min was set in order to reach the peak load value in 30 sec. Also a hold time of 10 sec was set at the maximum load value in order to diminish the contribution of creep on the indentation test results. An unloading rate of 60 mN/min was again employed before the indenter could be retracted from the samples. All micro-indentation tests were executed at room temperature with a maximum applied load of 30 mN. A total of five micro-indentation tests were carried out on each sample. These results were then averaged and recorded as the final value. An integrated microscope was used during each micro-indentation test to ensure proper placement of the indenter probe on undulation-free surfaces of the coatings to enhance the accuracy and repeatability of the test. The in-situ microscopic images of the coated surfaces were also recorded for each sample to visualize the extent of indentation at the maximum load.

3 Results and Discussion

3.1 FT-IR Analysis

When 10% ammonia solution was added to coating solutions of acrylic resin containing TEOS and these solutions were put under magnetic stirring, TEOS hydrolyzed to form three dimensional cross-linked silica clusters after condensation. This formation can be elucidated by the FT-IR spectra illustrated in Fig. 2. The Si-O-Si symmetrical stretching at ca. 800 cm^{-1}, Si-O-Si asymmetrical stretching at ca. 1020 cm^{-1} and Si-OH absorbance peak around 870 cm^{-1} confirm the presence of three dimensional cross-linked silica clusters. The intensities of these peaks are seen to increase with increasing TEOS content. A representation of the formation of three dimensional cross-linked silica structures can be illustrated through Fig. 3. Furthermore, the presence of acrylic resin in the coating material can be ascribed to the presence of C-H absorption peak at ca. 2920 cm^{-1}, C=O absorption peak at 1725 – 1745 cm^{-1} and C-O absorption peak at 1130 – 1170 cm^{-1}. The shift in absorption peak of C=O from ca. 1725 cm^{-1} in PAC-0 to ca. 1745 cm^{-1} in PAC-5, PAC-10 and PAC-15 also support possible hydrogen bonding between C=O groups of organic acrylic resin part and Si-OH. In addition, hydrogen bonding interactions can also be observed between C-O groups of organic acrylic resin part and Si-OH through the shift in absorption peak of C-O from ca. 1130 cm^{-1} in PAC-0 to ca. 1170 cm^{-1} in PAC-5, PAC-10 and PAC-15. Thus, it is anticipated that the acrylic resin also gets mingled with the silica clusters through formation of interpenetrating cross-linked structure upon drying (illustrated through Fig. 4). Moreover, TEOS also serves as the interaction sites connecting the organic acrylic resin to the inorganic three dimensional cross-linked silica clusters as shown in Fig. 5. This route not only enhances the adhesion of resin with the substrate but also influences the optical and hardness properties owing to the plausible hydrogen bonded sites in the organic acrylic resin and inorganic cross-linked silica structures as illustrated in Fig. 4 and 5.

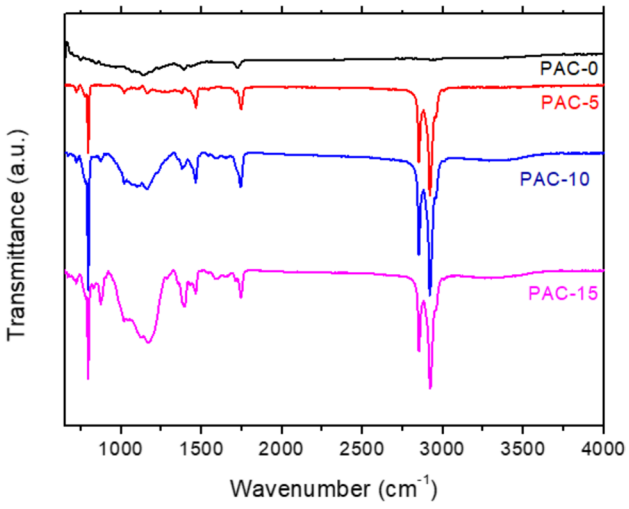

Fig. 2 Infrared spectra of coating materials

3.2 Coating Thickness

The coated coupon samples were analyzed for their dry coating thicknesses as the mechanical properties of the coating layer during indentation is affected by the mechanical properties of substrate if the depth of indentation is close to the thickness of the coating layer. A universal surface profilometer was chosen to measure the dry film thickness of the coating layer as it allows easy visualization of the thickness of dry coating layer as well as the smoothness of the coated surface. As a representative image, the dry coating thickness of PAC-15 coating formulation applied on PMMA substrate is exemplified in Fig. 6. It reveals that the approximate thickness of the dry film is 25 µm with a smooth surface finish. All the dry coating layers were observed to have thicknesses in the range of 22-25 µm (as shown in Fig. 7).

Furthermore, the roughness of dry coating surface is an important parameter so as to envisage the optical properties of the transparent protective coating as a rough or

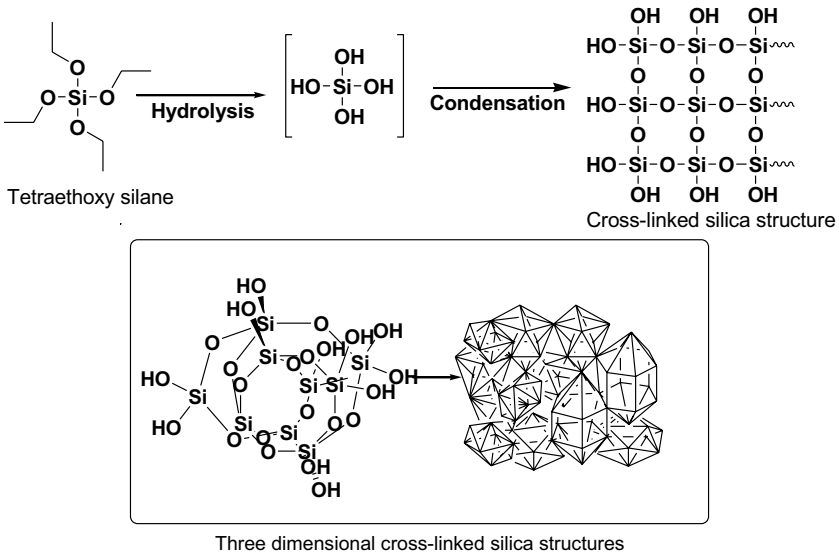

Fig. 3 Formation of cross-linked silica structures upon hydrolysis and condensation

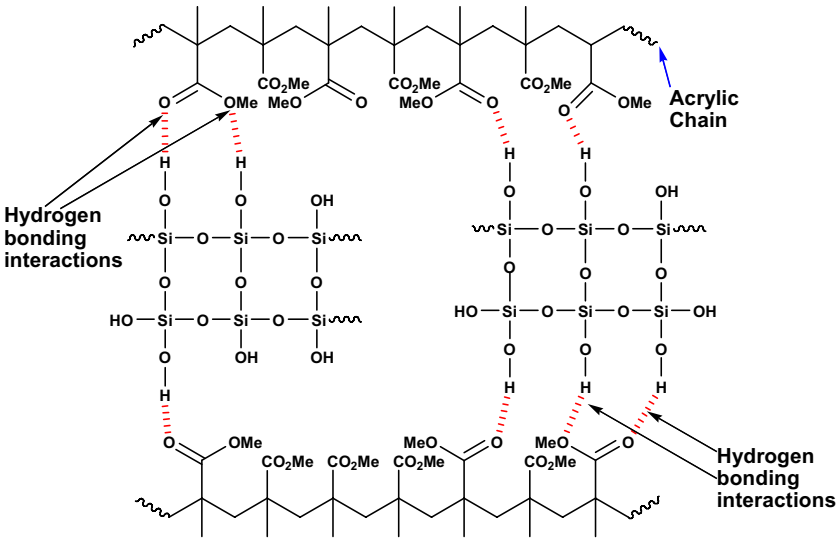

Fig. 4 Cross-linked silica and acrylic resin network

undulated surface would result in unwanted scattering of visible light. Thus, the smoothness and morphology of dry coating layer deposited on PMMA substrates were observed through SEM and the corresponding images have been illustrated in Fig. 8(a-d). It was evident that the surface was by and large smooth and free from major undulations even in the micrometer range. However, the outcome of TEOS addition on the morphology of dry coating layers can be clearly visualized through the cluster formation of cross-linked silica structures as revealed in the SEM micrographs particularly at a high TEOS content (typically in PAC-15). At a high loading of TEOS in PAC-15, some aggregates were seen to form whose sizes were observed to be in the micrometer range. Thus, TEOS content in excess of 15 wt.% is not anticipated to yield a coating with adequate transmittance because of the potential scattering of visible light by the micrometer sized cross-linked clusters of silica particles.

3.3 Optical Transmittance

Optical transmittance in the visible range of the electromagnetic spectrum (400 – 800 nm) is one of the most important criteria for selection of a protective coating for applications involving high level of transparency. Fig. 9 highlights the effect of TEOS addition on the transmittance of the acrylic resin formulations. As evident from Fig. 9, the transmittance of uncoated PMMA sample is not significantly altered by the application of TEOS modified acrylic resin coating formulations up to the TEOS content of less than 15% wt./wt. (with respect to the acrylic resin). Primarily, optical transparency of the coating is reported to be influenced by its surface

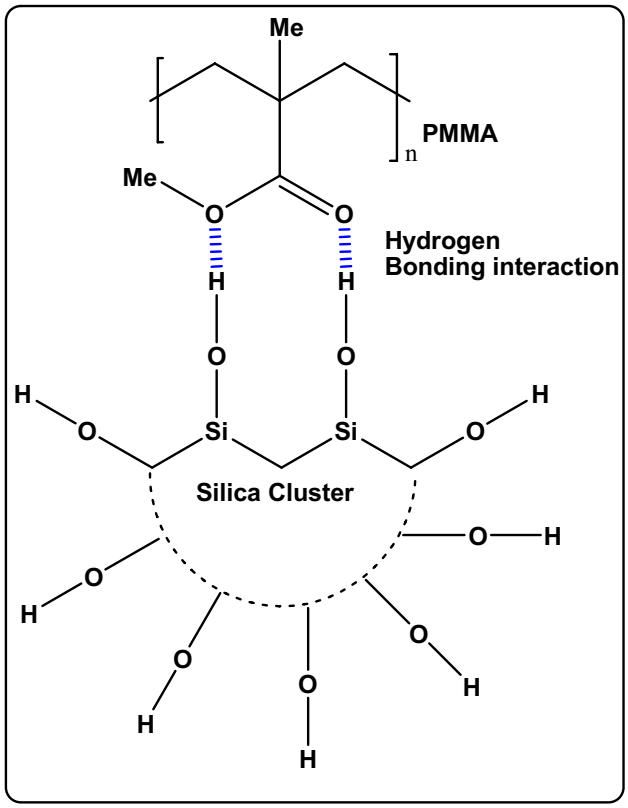

Fig. 5 Schematic representation of hydrogen bonding interaction between cross-linked silica cluster and acrylic resin

morphology. Thus, it was observed that the modified acrylic coating formulation PAC-15 which had 15% wt./wt. TEOS content demonstrated the least transmittance amongst all the samples tested in the visible range presumably due to the formation of micrometer sized aggregated clusters of cross-linked silica particles as depicted in Fig. 8(d). Similar results were also reported by Yao and co-workers [24] where they had observed that the optical transmittance of the samples had reduced from over 95% to ca. 85% with an increasing content of TEOS. They had reasoned that this was possibly because of SiO_2 microspheres which were not uniformly dispersed on the coating surface resulting in the reduced transparency. The current findings of this study are also in agreement with the results published by Zhao and co-workers [25] where it was observed that scattering of light by the agglomeration of NCC-SiO_2 hybrid colloids resulted in the loss of transparency in poly(acrylic acid) coatings. Furthermore, the findings observed in this study are also in conformity with the observations published by Chang and co-workers [26].

3.4 Instrumented Indentation

Instrumented indentation tests bring out the mechanical characteristics of the material directly from the indenter load and the depth of penetration, which are measured concurrently during the loading and unloading sequence and not predominantly from the direct observation of the imprint. Thus, instrumented indentation test provides additional information about material properties in comparison to the common hardness tests. The important material properties like Vickers hardness (H_v), indentation hardness (H_{IT}) and reduced modulus (E_r) obtained from instrumented indentation studies on the uncoated as well as coated PMMA substrates are illustrated in Table 1.

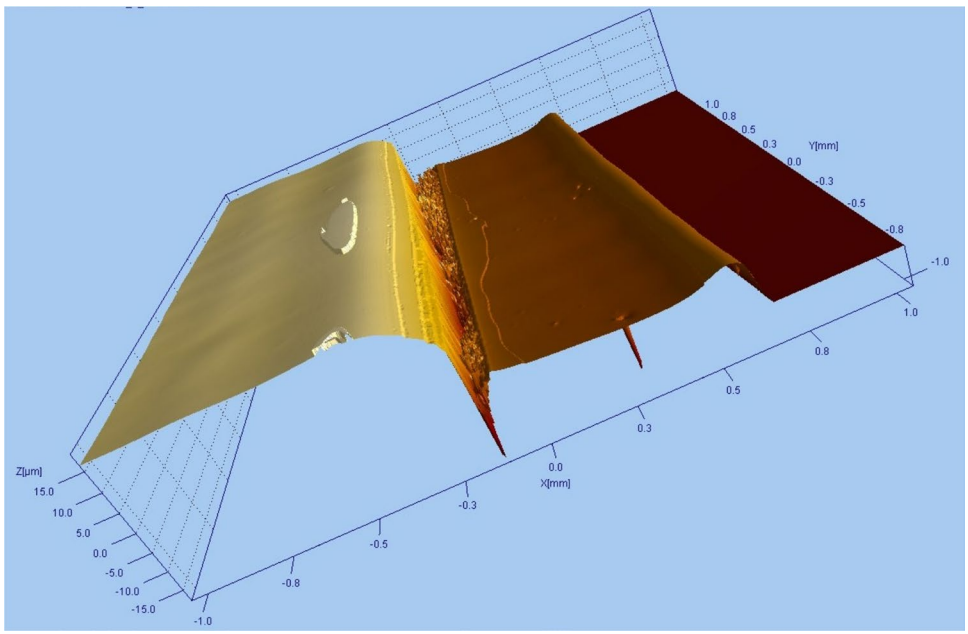

Fig. 6 Coating thickness of PAC-15 dry coating layer deposited on PMMA substrate visualized through a surface profilometer

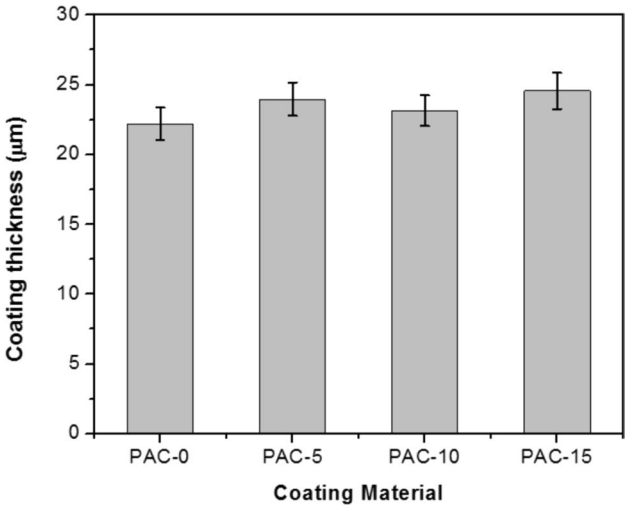

Fig. 7 Coating thicknesses of different materials' dry coating layer deposited on PMMA substrates

Vickers hardness (H_v) is generally obtained from the extent of the indentation created by a pyramid type diamond indenter with square base. The indenter's opposite sides meet at the top with an angle of 136°, the indenter's edges meet at 148° and the indenter's faces meet at 68°. H_v is estimated using the indentation load, P (in kgf) and the surface area of the impression, A_S using Eq. (1).

$$H_V = \frac{P}{A_S} = \frac{2P}{d^2}\sin\frac{136^0}{2} = 1.854\frac{P}{d^2} \tag{1}$$

In Eq. (1), 'd' is the length (in mm) of the diagonals from corner to corner of the indentation impression on the specimen surface. As evident from Table 1, the H_v values show a gradual increase from ca. 45 for PAC-0 to ca.71 for PAC-15, a net increase of approximately 56%. Subsequently H_v shows enhancement from ca. 31% in case of PAC-0 to about 105% in case of PAC-15 when compared to the uncoated PMMA sample. The increase in H_v values is supported by the micrographs illustrated in Fig. 10(a)-(e) whereby it can be seen that area of the indented impression was reduced with the increase in TEOS content presumably due to the increase in hardness of the coating layer.

The plots of load versus indentation depths of the uncoated and coated PMMA sample specimens (depicted in Fig. 11) have been utilized to gather important mechanical characteristics of the coatings. At a glance, it can be inferred that uncoated PMMA sample has the least resistance to indentation whereas PAC-15 coating demonstrates the highest resistance to indentation. Since the maximum indentation depth observed in the micro-indentation tests is less than 2 µm, it is less than 10% of the total thickness of the coating layer deposited on PMMA samples (Fig. 7). Consequently, it can be considered that the mechanical properties of the coating layer are not appreciably affected by the mechanical properties of PMMA substrate during instrumented indentation tests. Oliver and Pharr had devised a methodology to precisely calculate the indentation hardness (H_{IT}) and reduced modulus (E_r) of the samples from the indentation load and the indentation depth (or displacement) without the requirement of measuring the deformed area through a microscope [22]. In order to estimate indentation hardness (H_{IT}) and reduced modulus (E_r), the initial part of the load versus indentation depth values during the unloading segment were fitted to the power law type of model represented in Eq. (2) which was derived from the works of Oliver and Pharr [27]:

$$P = \beta(h - h_f)^m \tag{2}$$

The parameters 'β' and 'm' were determined by the curve fitting method, and h_f was the final displacement after the entire unloading stage which was also calculated from the curve fitting process. Then the contact stiffness (S) was determined through Eq. (3) by differentiation of the fitted curve of the unloading segment and estimating the outcome at $h = h_{max}$ where, h_{max} is the maximum indentation depth.

$$S = \left.\frac{dP}{dh}\right|_{h=h_{max}} = m\beta(h_{max} - h_f)^{m-1} \tag{3}$$

After evaluating 'S', the contact indentation depth 'h_C' was then evaluated from Eq. (4), which is less than the total indentation depth for an elastic material.

$$h_C = h_{max} - h_S \tag{4}$$

Here, 'h_S' is the amount of sink-in depth during the indentation test which can be estimated from Eq. (5), assuming that pile-up is negligible.

$$h_S = \varepsilon\frac{P_{max}}{S} \tag{5}$$

In Eq. (5), 'ε' is a geometric constant (≈ 0.727 for a Vickers indenter). Consequently, Eq. (4) can be transformed to Eq. (6).

$$h_C = h_{max} - \varepsilon\frac{P_{max}}{S} \tag{6}$$

Fischer-Cripps [28] has described a method to estimate the projected contact area (A_C) for a Vickers indenter from the contact indentation depth (h_C) using the relationship mentioned in Eq. (7).

$$A_C = 4h_c^2\tan^2\theta \tag{7}$$

If $\theta = 68°$ is incorporated in Eq. (7) for a Vickers indenter, A_C is further reduced to:

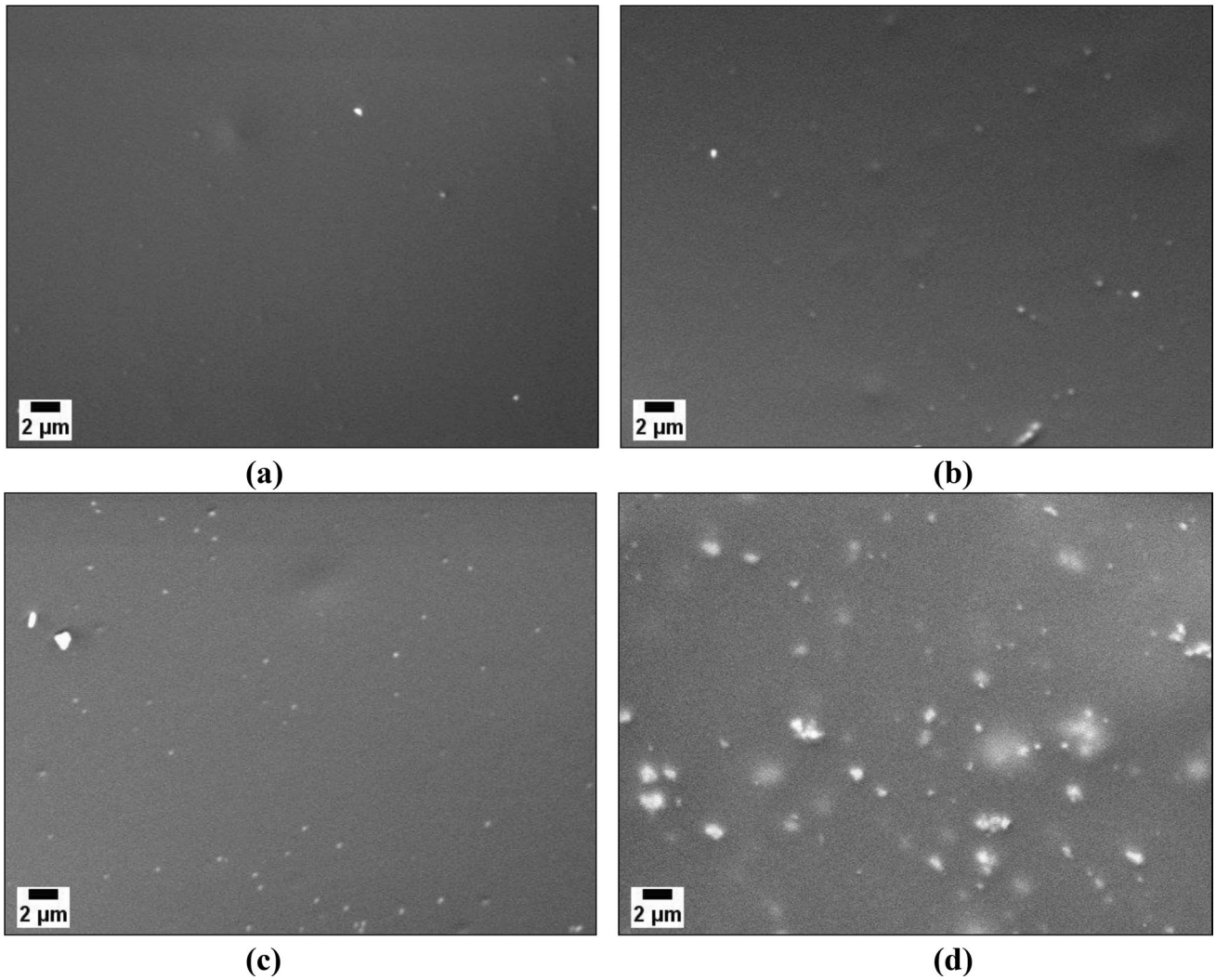

Fig. 8 SEM micrographs depicting surface smoothness and morphology of (**a**) PAC-0, (**b**) PAC-5, (**c**) PAC-10, and (**d**) PAC-15 coating formulations deposited on PMMA substrates

$$A_C = 24.504h_c^2 \tag{8}$$

Thus, H_{IT} can suitably be evaluated through Eq. (9) from the maximum applied load on the sample surface, P_{max} and estimated parameters like S, h_C and subsequently A_C:

$$H_{IT} = \frac{P_{max}}{A_C} \tag{9}$$

Much like the H_v values, H_{IT} values in Table 1 are also observed to be increased with an increase in the TEOS content (ca. 484 MPa for PAC-0 to ca. 759 MPa for PAC-15). Thus, there is more than 56% enhancement in H_{IT} when the TEOS content in the formulation is increased to 15 wt.%. Correspondingly, the indentation hardness shows improvement of more than 30% in case of PAC-0 to about 105% in case of PAC-15 when compared to uncoated PMMA sheet which is similar to the trend observed for Vickers hardness values. Therefore, it was observed that TEOS significantly improved the hardness of the coating formulation through the formation of cross-linked silica structures. This inference also agrees with the findings reported by Lorenzo et al. [23] and Yao and co-workers [24].

Oliver and Pharr (O&P) method [22] also facilitates the estimation of experimentally observed elastic modulus through the instrumented indentation experiments. The indentation elastic modulus of materials generally represented by the reduced modulus (E_r) can be calculated from Eq. (10).

$$E_r = \frac{S\sqrt{\pi}}{2B\sqrt{A_C}} \tag{10}$$

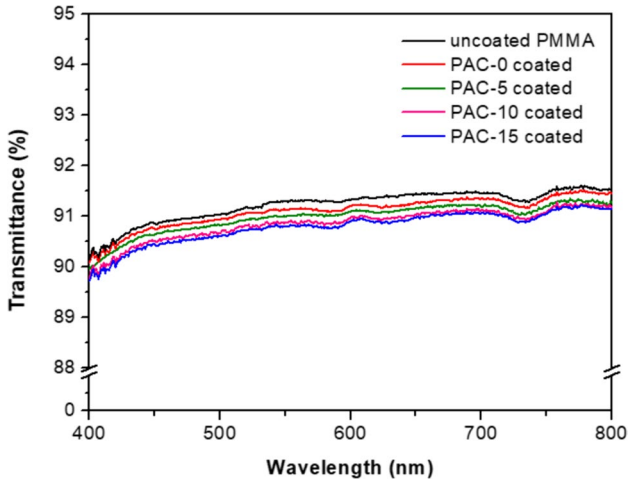

Fig. 9 Optical transmittance of PMMA samples coated with varied coating formulations in comparison to that of the uncoated PMMA sample

where, '*B*' is the tip geometry correction factor which is ideally 1.012 for a Vickers indenter [28]. E_r is an estimate of how efficiently a material is able to transfer the applied load between its micro-structural phases without undergoing significant deformation. As observed in Table 1, E_r is only enhanced by ca. 16% when the unmodified coating formulation (PAC-0) is applied on the PMMA sample, primarily due to the superior molecular rigidity of coating material, as compared to uncoated PMMA. Subsequently, when the modified acrylic formulation PAC-15 is applied on the same substrate, the corresponding enhancement is more than 90% suggesting strong interactions between the organic-inorganic phases. Moreover, when Eq. (10) is scrutinized, it can be seen that E_r is directly dependent on the contact stiffness of the coating material (S). Fig. 12 suggests that addition of TEOS in the coating formulation improves the stiffness of the coating material (almost up to 150% in case of the modified acrylic formulation PAC-15 when compared to the unmodified acrylic formulation PAC-0) which may be ascribed to strong interactions between the acrylic resin chain segments and the cross-linked silica structures.

The indentation depth versus time plot (Fig. 13) gives valuable information about the viscoelastic nature of the coating layer. Keeping the indenter tip at hold for some time permits the relaxation processes (which is time-dependent) to take place and this procedure diminishes the residual stresses in the material. The indenter tip during this time penetrates in the material and the depth of penetration is an indication of the material's viscous nature. It is evident from Fig. 13 that all the coating formulations show significant viscoelastic behavior. However, the viscous nature of coating formulation is observed to decrease when the TEOS content in the coating formulation increases, as evident from Fig. 14 where it is seen that the indenter displacement at holding is maximum for the unmodified acrylic formulation PAC-0 and least for the modified acrylic formulation PAC-15. Conversely, the material free from TEOS (i.e. PAC-0) shows the least elastic nature whereas the modified acrylic formulation PAC-15 displays the most elastic nature which can again be attributed to the increasing order of hydrogen bonding interactions between the organic-inorganic phases due to the presence of free hydroxy groups on the surface of silica clusters and ethereal and carbonyl oxygen of PMMA (as depicted in Fig. 4 and 5). The extent of creep can also be estimated from the displacement observed during the holding stage when the load is kept constant for some time. From Fig. 14 it is evident that the extent of creep is lowered with the addition of TEOS in the coating formulations primarily due to the interacting organic and inorganic phases in the coating material which reduces the viscous nature of the material.

The comparison between plastic contact depth (also termed as the indentation contact depth, h_C) and elastic displacement (also termed as the sink-in depth, h_S) of the coating formulations containing different percentages of TEOS is depicted in Fig. 15. Here, plastic contact depth (h_C) is observed to be reduced significantly with the addition of TEOS in comparison to the elastic displacement (h_S). In this study, h_S is seen to effectively remain constant throughout the loading-unloading processes of the micro-indentation test while the addition of TEOS in the acrylic resin formulation had resulted in the reduction of plastic contact depths (h_C) for all the pertinent coating formulations. This observation again supports the improved hardness as well as modulus of the TEOS containing coating formulations, owing to the formation of three dimensional cross-linked

Table 1 Mechanical properties, like Vickers hardness (H_v), indentation hardness (H_{IT}) and reduced modulus (E_r), of the uncoated and coated PMMA substrates, obtained through the instrumented indentation test

Material	TEOS (% wt./wt.)	H_v (Vickers)	H_{IT} (MPa)	E_r (GPa)
Uncoated PMMA	--	34.93 ± 4.53	370.07 ± 47.95	6.74 ± 0.25
PAC-0	0	45.74 ± 2.52	484.59 ± 26.71	7.84 ± 0.39
PAC-5	5	55.01 ± 4.22	592.84 ± 44.76	9.55 ± 1.92
PAC-10	10	57.16 ± 4.33	605.57 ± 45.94	10.38 ± 0.51
PAC-15	15	71.65 ± 4.49	759.11 ± 53.57	12.96 ± 1.24

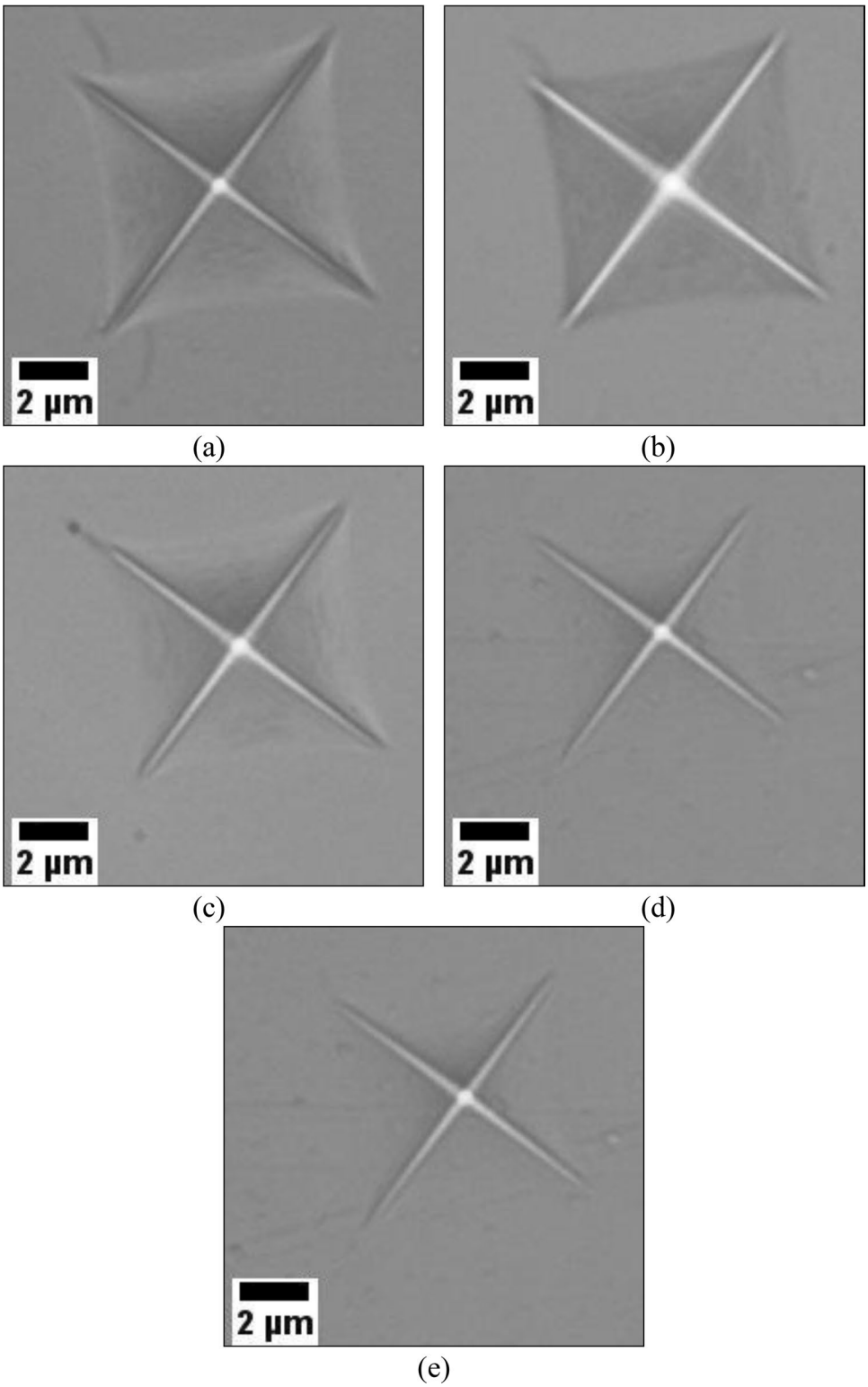

Fig. 10 Impressions created by the Vickers indenter in (**a**) uncoated PMMA, and (**b**) PAC-0, (**c**) PAC-5, (**d**) PAC-10, (**e**) PAC-15 coated PMMA substrates during the micro-indentation tests

silica structures coupled with the strong interactions between organic and inorganic phases of the coating, when deposited on the PMMA samples and allowed to dry in the optimum condition. Thus, evaluation of mechanical properties through instrumented indentation method is observed to significantly offer a pragmatic understanding of the effect of the inorganic phase on hardness, modulus, stiffness and viscoelastic properties of the silane modified acrylic based hybrid coatings, which corroborated well with microscopic evidences.

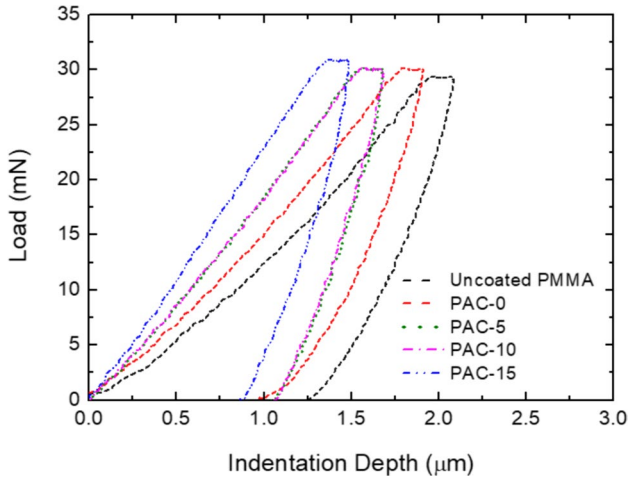

Fig. 11 Indentation depth profiles of the substrate and the coating materials

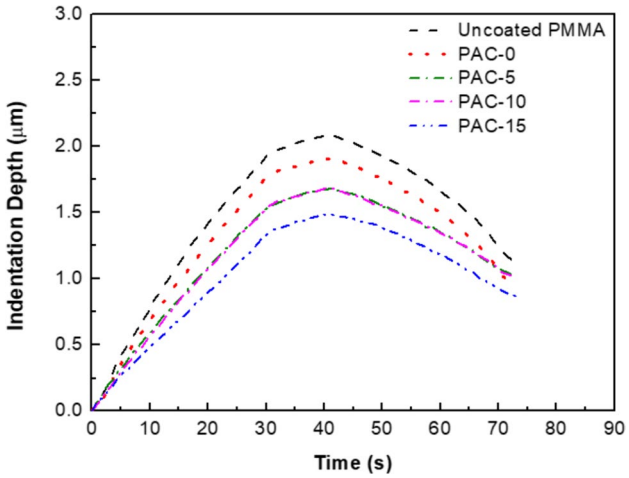

Fig. 13 Time dependent indentation depth profiles of the substrate and the coating materials

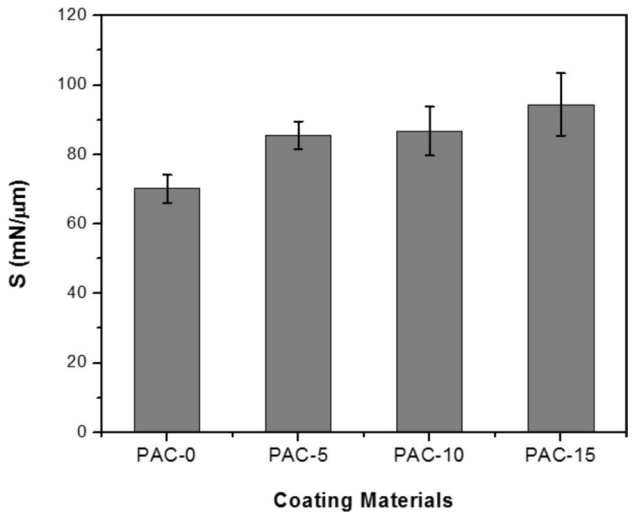

Fig. 12 Contact stiffness (*S*) of different coating materials deposited on PMMA substrates

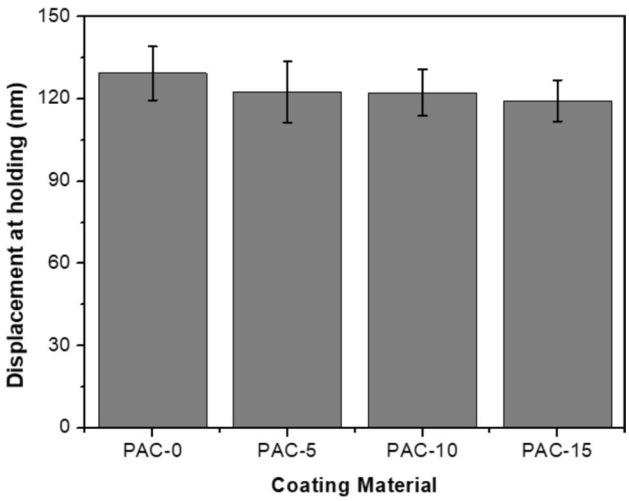

Fig. 14 Displacement of the indenter tip during holding time for samples containing different amounts of TEOS

3.5 Wet Abrasion Test

Transmittance (*Tr*) and haze (*Haze*) values of the uncoated and coated PMMA sample specimens, before (Tr_B, $Haze_B$) and after (Tr_A, $Haze_A$) the wet abrasion test respectively have been elucidated in Table 2. It is anticipated that there will be a marked loss in transmittance values of the samples supplemented by an increase in the haze values when the samples undergo the wet abrasion tests. In the present study, the uncoated PMMA sample specimen shows a decline in transmittance value from ca. 92% to ca. 88% (decrease in ca. 4%) when subjected to the wet abrasion test. Contrary to this, all the coated PMMA sample specimens using the acrylic coating formulations show loss of less than 1% in the transmittance values before and after the wet abrasion tests. However, the haze values of the coated sample specimens show noticeable increase after the wet abrasion test. Since haze is quantified as the ratio of the diffused transmittance and the total transmittance observed through the sample, it can evidently indicate the amount of light being diffused or scattered by the sample. Thus, the sample which has undergone more abrasion is expected to diffuse/ scatter light more than the sample which has undergone less abrasion. Consequently the difference in haze values of the samples evaluated before and after the wet abrasion test can indicate the coating layer's scratch resistance. In this study, it was observed that the haze value of uncoated PMMA sample was increased to ca. 8% after the wet abrasion test in comparison to ca.

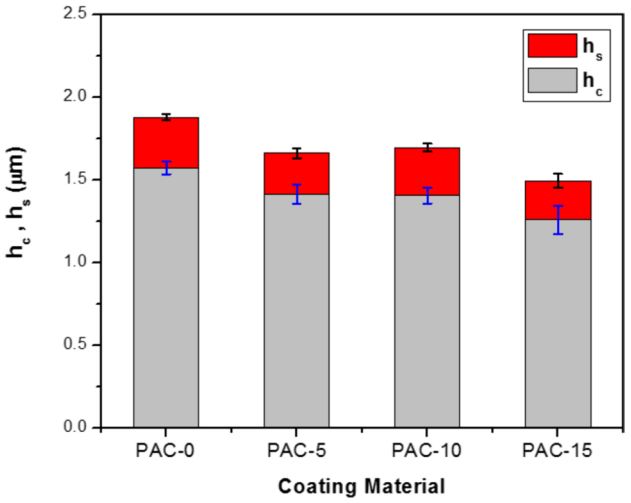

Fig. 15 Elastic displacement (h_S) and plastic contact depth (h_C) as the function of TEOS content in the coating materials

1% haze value obtained before the wet abrasion test indicating an increment of over 7%. In case of the unmodified acrylic formulation (PAC-0), it was further seen that this increment was of approximately 4.6%. On the other hand, in case of the modified acrylic formulation PAC-5 it was observed that this increment in haze due to the wet abrasion test was brought down to roughly 1.54% owing to the increased hardness of the coating layer and thus points to a better scratch resistance of the coating layer in comparison to the unmodified acrylic formulation (PAC-0). Similarly, in case of the modified acrylic formulation PAC-10 the increase in haze value was observed to be approximately of the same order (ca. 1.83%). However, in case of the modified acrylic formulation PAC-15 it was noticed that this increment in haze due to abrasion was again increased to approximately 2.78% potentially due to the combined effects of abrasion and the presence of micrometer sized aggregated clusters of cross-linked silica particles as revealed in Fig. 8(d). Thus, it is apparent that the abrasion/ scratch resistance is in coherence with the physico-mechanical properties of the coating formulations and also agrees with the morphological features of the coating layers.

4 Conclusions

Through this study, the effect of TEOS addition in the acrylic resin formulation to prepare acrylic resin based organic-inorganic hybrid transparent protective coating formulations for probable use on PMMA substrates was brought out, primarily with respect to the optical properties (transmittance and haze), wet abrasion resistance and most prominently the mechanical properties under instrumented indentation. The salient corollaries of the present study are:

1. TEOS was essentially used in the coating solution to produce organic-inorganic hybrid materials which could be used as transparent protective hard coats when hydrolyzed and cross-linked. TEOS not only forms cross-linked silica structures but also facilitates the development of interlinks between the acrylic resin chains and the inorganic phase due to the hydrogen bonding interactions.
2. Hardness, stiffness and reduced elastic modulus of the coating materials were observed to get enhanced with the addition of TEOS (up to ca. 56%, 28% and 65% respectively in case of the modified acrylic coating formulation PAC-15). When compared to the uncoated PMMA sample, the hardness as well as the reduced elastic modulus of hybrid coatings showed improvements up to ca. 105% and 90% respectively. The elastic nature of coating materials moreover increased with the addition of TEOS. These enhancements in mechanical properties were ascribed to strong interactions between the organic and inorganic components of the coating material and also to the concurrent formation of cross-linked silica structures. These results were aptly supported by microscopy images.
3. The developed hard coats demonstrated less than 0.5% loss in transmittance when compared to uncoated PMMA thus retaining the excellent optical transmittance of PMMA sample ($\geq$ 90% transmission in 400 – 800 nm wavelength).
4. TEOS addition in the acrylic coating formulations further resulted in enhanced wet abrasion resistance (and

Table 2 Transmittance (*Tr*) and Haze (*Haze*) values of the uncoated and coated PMMA substrates, before (Tr_B, $Haze_B$) and after (Tr_A, $Haze_A$) wet abrasion test respectively

Material	TEOS (% wt./wt.)	Tr_B (%)	Tr_A (%)	$Haze_B$ (%)	$Haze_A$ (%)
Uncoated PMMA	--	92.49 ± 0.02	88.31 ± 1.05	1.36 ± 0.26	7.67 ± 0.98
PAC-0	0	92.48 ± 0.01	92.20 ± 0.08	0.82 ± 0.19	5.46 ± 0.75
PAC-5	5	92.46 ± 0.02	92.44 ± 0.04	0.55 ± 0.21	2.09 ± 0.37
PAC-10	10	92.42 ± 0.03	92.31 ± 0.15	1.02 ± 0.49	2.85 ± 0.41
PAC-15	15	92.31 ± 0.03	92.19 ± 0.16	1.14 ± 0.48	3.92 ± 0.60

consequently enhanced scratch resistance) of the coatings as revealed by their optical properties (transmittance and haze) before and after the wet abrasion tests. These results augur well with the physico-mechanical properties of the coating formulations. However, TEOS content of more than 15 wt.% is anticipated to produce a coating with inadequate optical clarity because of the potential scattering of visible light by the micrometer sized cross-linked silica clusters.

Consequently, the assessed parameters are some of the most important attributes of a protective coating required for highly transparent PMMA substrates for various applications.

Acknowledgements The authors are grateful to Dr. Mayank Dwivedi, Outstanding Scientist and Director, DMSRDE Kanpur for providing necessary guidance and support to accomplish the reported work. The authors would also like to extend their gratitude to all the members of Polymers and Rubber Division of DMSRDE for providing necessary help and assistance to execute this work. The authors would also like to thank Dr. Kavita Agarwal and Mr. Rakesh Kumar for SEM analysis as well as Mr. Shilendra Kumar and Dr. Sunil Kumar for the wet abrasion tests. The authors would like to furthermore thank Prof. Kantesh Balani for extending the instrumented indentation facility at Indian Institute of Technology Kanpur for this research work.

Authors' Contributions Vishal Das (V.D.) contributed to: study conception and design; material preparation, data collection and analysis; preparation of the first draft of the manuscript.

Dr. Ajit Shankar Singh (A.S.S.) contributed to: study conception and design; material preparation, data collection and analysis.

Abhishek Singh (A.S.) contributed to: material preparation, data collection and analysis.

Preeti Mishra (P.M.) contributed to: material preparation, data collection and analysis.

Dr. Dibyendu Sekhar Bag (D.S.B.) contributed to: study conception and design; review and revision of the manuscript.

All the authors commented on previous versions of the manuscript. All authors read and approved the final manuscript.

Funding The authors declare that no funds, grants, or other support were received during the preparation of this manuscript.

Data Availability All data generated or analyzed during this study are included in this article.

Declarations

Ethics Approval Not Applicable.

Consent to Participate Not Applicable.

Consent for Publication Not Applicable.

Competing Interests The authors declare no competing interests.

References

1. Wang X, Wei S, Xu B, Chen Y, Yan X, Xia H (2015) Transparent organic materials of aircraft cockpit canopies: research status and development trends. Mater Res Innov 19(10):S10-199-S10-206
2. Barroso G, Li Q, Bordia RK, Motz G (2019) Polymeric and ceramic silicon-based coatings – a review. J Mater Chem A 7(5):1936–1963
3. Ranjbar Z, Rastegar S (2011) Nano mechanical properties of an automotive clear-coats containing nano silica particles with different surface chemistries. Prog Org Coat 72(1–2):40–43
4. Zhou S, Wu L, Sun J, Shen W (2002) The change of the properties of acrylic-based polyurethane via addition of nano-silica. Prog Org Coat 45(1):33–42
5. Tahmassebi N, Moradian S, Ramezanzadeh B, Khosravi A, Behdad S (2010) Effect of addition of hydrophobic nano silica on viscoelastic properties and scratch resistance of an acrylic/melamine automotive clearcoat. Tribol Int 43(3):685–693
6. Gläsel HJ, Bauer F, Ernst H, Findeisen M, Hartmann E, Langguth H, Mehnert R, Schubert R (2000) Preparation of scratch and abrasion resistant polymeric nanocomposites by monomer grafting onto nanoparticles - 2: characterization of radiation-cured polymeric nanocomposites. Macromol Chem Phys 201(18):2765–2770
7. Cho JD, Ju HT, Hong JW (2005) Photocuring kinetics of UV-initiated free-radical photopolymerizations with and without silica nanoparticles. J Polym Sci A Polym Chem 43(3):658–670
8. Jalili MM, Moradian S, Dastmalchian H, Karbasi A (2007) Investigating the variations in properties of 2-pack polyurethane clear coat through separate incorporation of hydrophilic and hydrophobic nano-silica. Prog Org Coat 59(1):81–87
9. Bauer F, Ernst H, Decker U, Findeisen M, Gläsel HJ, Langguth H, Hartmann E, Mehnert R, Peuker C (2000) Preparation of scratch and abrasion resistant polymeric nanocomposites by monomer grafting onto nanoparticles – 1: FTIR and multi-nuclear NMR spectroscopy to the characterization of methacryl grafting. Macromol Chem Phys 201(18):2654–2659
10. Bauer F, Ernst H, Hirsch D, Naumov S, Pelzing M, Sauerland V, Mehnert R (2004) Preparation of scratch and abrasion resistant polymeric nanocomposites by monomer grafting onto nanoparticles - 5. Macromol Chem Phys 205(12):1587–1593
11. Bauer F, Flyun R, Czihal K, Buchmeiser MR, Langguth H, Mehnert R (2006) Nano/micro particle hybrid composites for scratch and abrasion resistant polyacrylate coatings. Macromol Mater Eng 291(5):493–498
12. Ahmad S, Gupta AP, Sharmin E, Alam M, Pandey SK (2005) Synthesis, characterization and development of high performance siloxane-modified epoxy paints. Prog Org Coat 54(3):248–255
13. Sangermano M, Messori M (2010) Scratch resistance enhancement of polymer coatings. Macromol Mater Eng 295(7):603–612
14. Omrani A, Afsar S, Safarpour MA (2010) Thermoset nanocomposites using hybrid nano TiO_2–SiO_2. Mater Chem Phys 122(2–3):343–349
15. Ferchichi A, Calas-Etienne S, Smaïhi M, Prévot G, Solignac P, Etienne P (2009) Relation between structure and mechanical properties (elastoplastic and fracture behavior) of hybrid organic–inorganic coating. J Mater Sci 44(11):2752–2758
16. Larson KL, Pare SM, Sundaram VS (2011) Barrier coatings for polymeric substrates. United States patent US 7,878,054. 2011 Feb 01
17. Coak CE, Sundaram VS, Wascher WW (2012) Durable transparent coatings for aircraft passenger windows. United States patent US 8,313,812. 2012 Nov 20
18. Larson-Smith KL, Sundaram VS, Sirkis MR (2009) Wear resistant coating for polymeric transparencies. United States patent application US 12/137,390. 2009 Dec 17
19. Coak CE, Sundaram VS, Wascher WW (2007) Durable transparent coatings for polymeric substrates. United States patent application US 11/696,661. 2007 Aug 23
20. Qi Y, Xiao ZG, Mantei TD (2003) Comparison of silicon dioxide layers grown from three polymethylsiloxane precursors in a high-density oxygen plasma. J Vac Sci Technol A 21(4):1064–1068

21. Doerner MF, Nix WD (1986) A method for interpreting the data from depth-sensing indentation instruments. J Mater Res 1(4):601–609
22. Oliver WC, Pharr GM (1992) An improved technique for determining hardness and elastic modulus using load and displacement sensing indentation experiments. J Mater Res 7(6):1564–1583
23. Lorenzo V, Acebo C, Ramis X, Serra À (2016) Mechanical characterization of sol–gel epoxy-silylated hyperbranched poly(ethyleneimine) coatings by means of Depth Sensing Indentation methods. Prog Org Coat 92:16–22
24. Yao B, Zhao H, Wang L, Liu Y, Zheng C, Li H, Sun C (2018) Synthesis of acrylate-based UV/thermal dual-cure coatings for antifogging. J Coat Technol Res 15(1):149–158
25. Zhao G, Ding C, Pan M, Zhai S (2018) Fabrication of NCC-SiO_2 hybrid colloids and its application on waterborne poly(acrylic acid) coatings. Prog Org Coat 122:88–95
26. Chang CC, Wu YT, Cheng LP (2016) Preparation of HMDS-modified silica/polyacrylate hydrophobic hard coatings on PMMA substrates. J Coat Technol Res 13(6):999–1007
27. Oliver WC, Pharr GM (2004) Measurement of hardness and elastic modulus by instrumented indentation: advances in understanding and refinements to methodology. J Mater Res 19(1):3–20
28. Fischer-Cripps AC (2011) Nanoindentation. Springer, New York